

# IMPROVING THE MAPPING AND PREDICTION OF OFFSHORE WIND RESOURCES (IMPOWR)

## Experimental Overview and First Results

BY BRIAN A. COLLE, MATTHEW J. SIENKIEWICZ, CRISTINA ARCHER, DANA VERON, FABRICE VERON, WILLETT KEMPTON, AND JOHN E. MAK

The IMPOWR field program collected surface, tower, and aircraft observations over coastal southern New England, which will broaden our understanding of diurnal coastal flows and improve models for offshore wind power.

**T**he coastal waters of the Northeast United States are an ideal location for developing offshore wind power given the combination of large wind resource, high population density, and shallow coastal bathymetry (Kempton et al. 2007; Dvorak et al. 2012b). Archer et al. (2014) identified three main areas of opportunity for facilitating offshore wind

farm development through better meteorological observations and atmospheric modeling: 1) enhancing offshore wind resource assessment, 2) improving wind power forecasting, and 3) characterizing turbulent wake losses of wind farms. There are other challenges to developing offshore wind power, such as design of support structures, transmission, and interconnection to the power system; the trade-off between locating farther from shore to reduce visual impact and increase wind speed versus locating closer to shore for lower construction cost; environmental assessment; and financing, power purchase contracts, infrastructure, and supply chain development to reduce cost of electricity, among others. However, while relevant, they are not the subjects of this article.

There have been several wind resource assessments along the Northeast U.S. coastal waters (Manwell et al. 2002; Musial and Ram 2010; Dvorak et al. 2012a; Woods et al. 2013; Monaldo et al. 2014). Wind resource assessment in coastal and offshore areas currently suffers from a lack of observations at turbine hub height (i.e., around 100 m above mean water level); thus, the need for more multilevel observations

**AFFILIATIONS:** COLLE AND SIENKIEWICZ—School of Marine and Atmospheric Sciences, Stony Brook University, Stony Brook, New York; ARCHER, D. VERON, F. VERON, AND KEMPTON—College of Earth, Ocean, and Environment, University of Delaware, Newark, Delaware; MAK—UltraPure Air LLC, Setauket, New York

**CORRESPONDING AUTHOR:** Dr. Brian A. Colle, School of Marine and Atmospheric Sciences, Stony Brook University, Stony Brook, NY 11794-5000

E-mail: brian.colle@stonybrook.edu

*The abstract for this article can be found in this issue, following the table of contents.*

DOI:10.1175/BAMS-D-14-00253.1

In final form 28 October 2015

©2016 American Meteorological Society

of wind and temperature on offshore platforms was identified (Archer et al. 2014). Improved understanding and realistic modeling of coastal processes are also necessary for accurate wind resource assessment and wind forecasting, yet current numerical weather prediction models and their parameterizations of the planetary boundary layer (PBL) have not been comprehensively evaluated in this offshore area. Since the power available in the wind is proportional to the cube of wind speed, small wind speed forecast errors can result in large errors in the prediction of the available power. Accurate representation of mesoscale and synoptic-scale processes is important for resource assessment and return on investment planning prior to construction as well as to operational forecasts such as hour-ahead and day-ahead power production forecasts, upon which unit commitment and scheduling decisions are based.

There are important diurnal circulations near the Northeast coast during the warm season, such as sea breezes (Hughes and Veron 2015; Novak and Colle 2006; Colby 2004) and low-level jets (LLJs). Colle and Novak (2010) showed the existence of a diurnally

forced LLJ in the New York Bight region that often consisted of winds with speeds in excess of  $13 \text{ m s}^{-1}$ . Other LLJs have been documented along the U.S. East Coast associated the sloping Appalachians and coastal temperature boundaries along the mid-Atlantic during the warm season (Zhang et al. 2006; Ryan 2004) and low-level temperature boundaries near the coast during the cool season (Doyle and Warner 1991). Occurrences of the New York Bight jet peak on days in the late springtime when the land–sea temperature contrast is the greatest and when the flow is primarily southwesterly around a Bermuda high pressure system. The southerly LLJs over the southern Great Plains develop under similar synoptic conditions (Bonner 1968), with surface high pressure situated to the east of the plains. The New York Bight jet maxima were found to occur at about 150 m above mean sea level (MSL), just above hub height of a typical offshore wind turbine, and were part of a larger-scale coastal wind enhancement in the southern New England region. Helmis et al. (2013) also confirmed the presence of several summertime LLJ structures above Nantucket, Massachusetts, using various observational datasets.

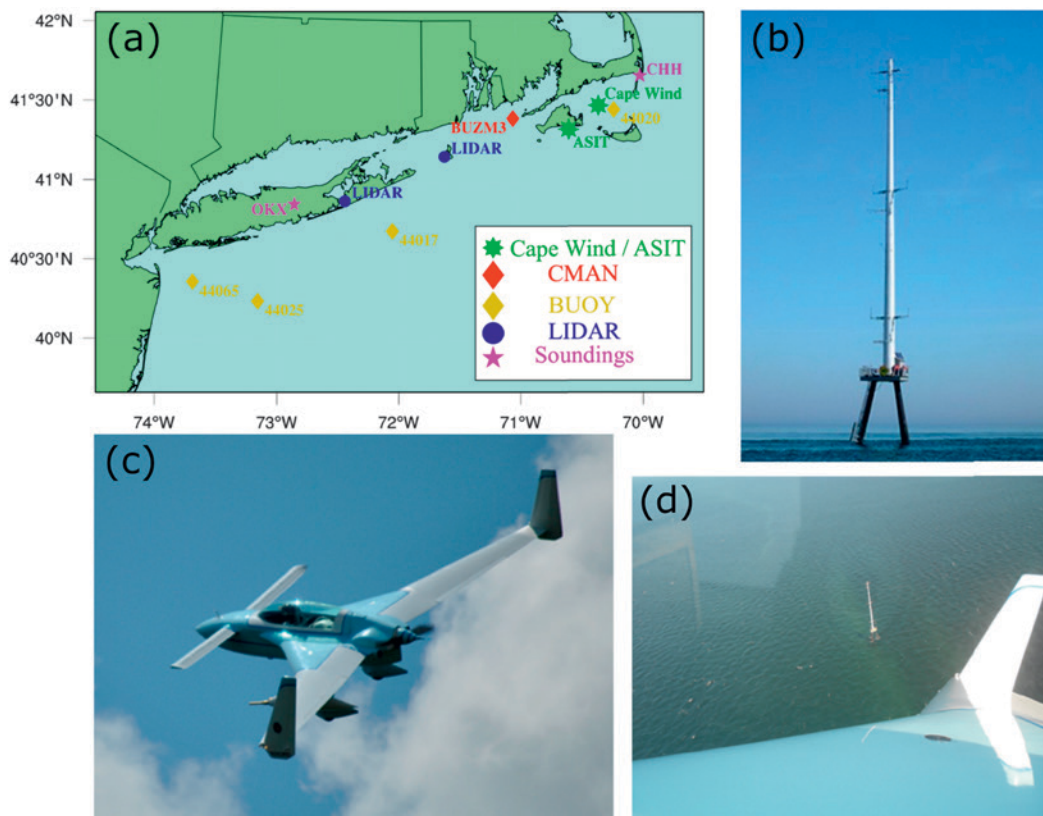


**FIG. 1.** (a) Map of the IMPOWER observations used in the region. Photos of (b) the Cape Wind tower [green star in (a)], (c) Long-EZ aircraft that was deployed from near Westhampton Beach (FOK) on Long Island, and (d) a spiral of the Long-EZ over the Cape Wind tower. Photos credits: Dana Veron for (b), John Mak for (c), and Matthew Sienkiewicz for (d).

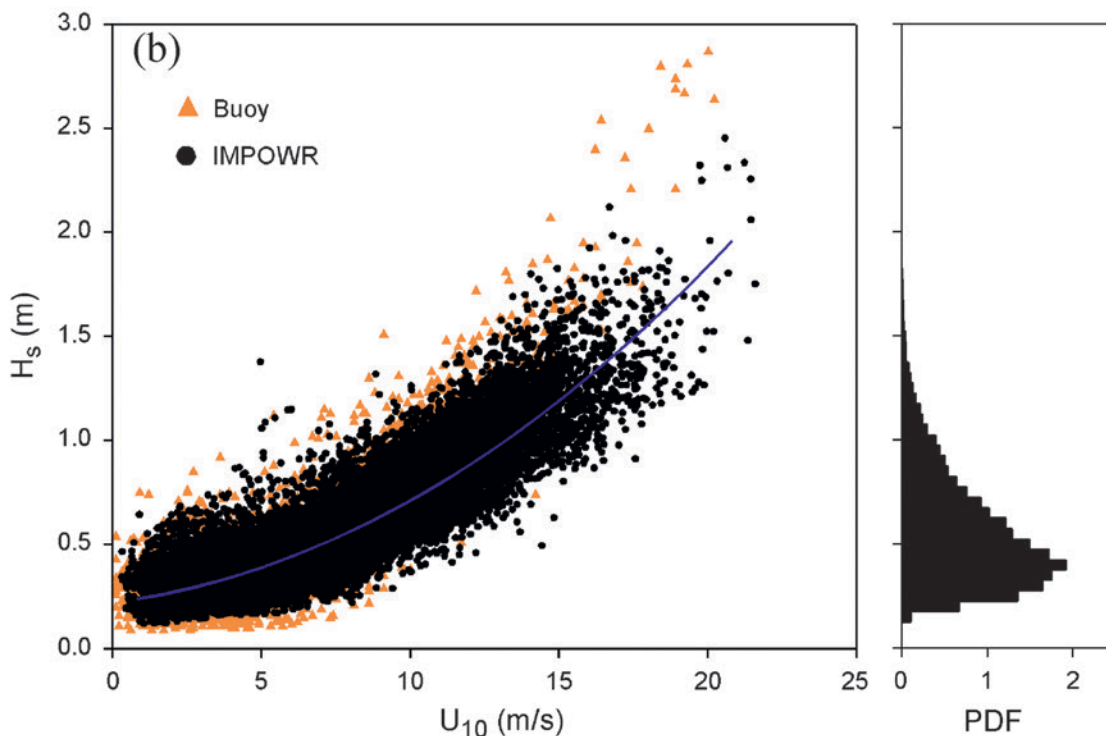
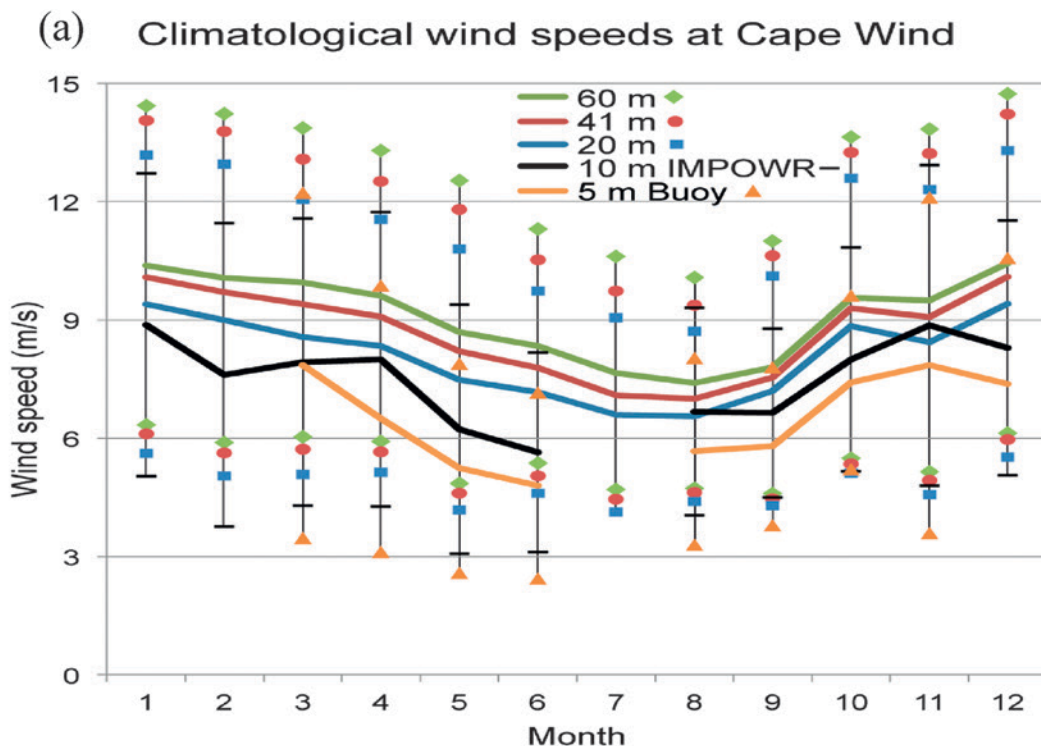
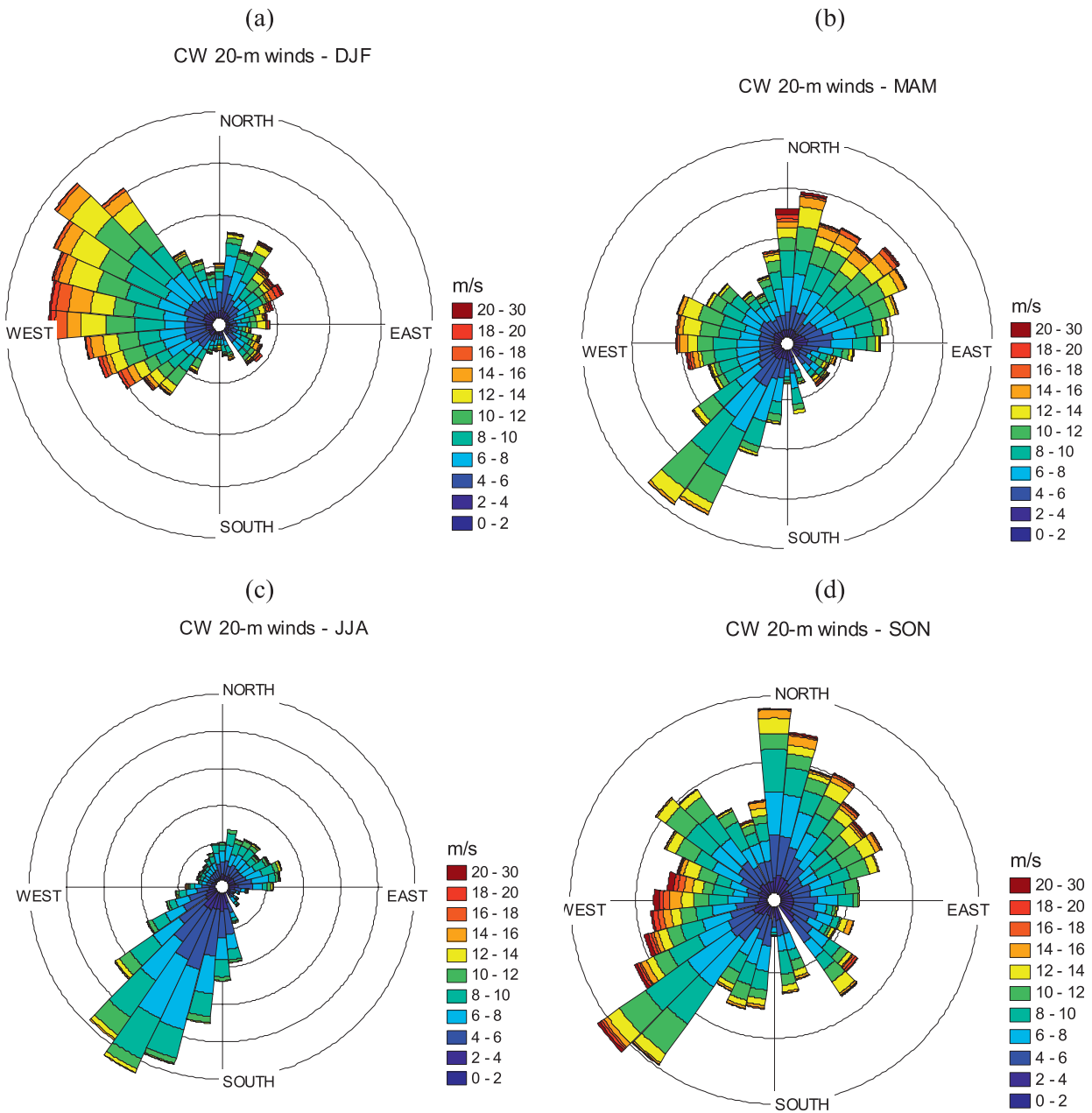


FIG. 2. Examples of data collected around the Cape Wind tower showing the (a) average wind speed ( $\text{m s}^{-1}$ ) at 20-, 41-, and 60-m levels at the tower during 2003–07, at 10 m from IMPOWR anemometers in 2013/14 on the tower platform, and at 5 m from nearby buoy 44020 during IMPOWR anemometers' available times, with markers indicating one standard deviation, and (b) significant wave height ( $H_s$  in meters) vs 10-m wind speed from the buoy and 10-m IMPOWR anemometer in 2013/14. The right shows the frequency of occurrence [probability density function (PDF)] of significant wave heights in  $dH_s = 0.1$  m bins. The significant wave height most frequently observed is approximately 0.4 m. The PDF is normalized such that  $\int \text{PDF} dH_s = 1$ .



**FIG. 3. Seasonal wind roses from the CW tower at 20 m during 2003–07 for (a) Dec–Feb, (b) Mar–May, (c) Jun–Aug, and (d) Sep–Nov. Frequency intervals are 1% per line.**

**MOTIVATION.** Mesoscale model verification efforts for offshore wind power across western Europe have used tall mast (~100 m), wind lidar, and satellite data. Carvalho et al. (2014a) and Hahmann et al. (2015) showed that Weather Research and Forecasting (WRF) Model surface winds are sensitive to the PBL and surface-layer parameterizations employed as well as to the reanalysis used. Even with these potential uncertainties, WRF-simulated wind data have been shown to be the best alternative to observed in situ offshore wind data (Carvalho et al. 2014b).

There has been limited verification of models near hub height (~100 m) over the coastal Northeast United States, given the scarcity of observations of the marine boundary layer in this marine environment. This region, stretching from the south shore of Long Island to Georges Bank, has been identified by Dvorak et al. (2012b) as an ideal location for an offshore wind energy grid based on available wind resource, regional energy demand, and shallow water depth. Previous studies have utilized available surface, sounding, and short-tower observations to validate WRF. Woods

**TABLE 1. Flight days for the IMPOWR field experiment.**

Flight day	Weather conditions
12 Nov 2012	Cyclone warm sector with south winds
4 Apr 2013	Southwest flow around anticyclone
7 Apr 2013	Stable strong south flow ahead of warm front
9 Apr 2013	Southwest flow ahead of cold front
4 May 2013	Moderate northeast flow with a subsidence inversion at top of PBL
10 May 2013	Southwest flow with coastal sea breezes
16 May 2013	Southwest flow with coastal jet
20 Jun 2013	Coastal sea breeze with westerly flow aloft
21 Jun 2013	Coastal sea breeze with westerly flow aloft
23 Jun 2013	Southwesterly flow with coastal flow enhancement
24 Jun 2013	Weak New York Bight jet event
28 Sep 2013	Northeasterly flow around anticyclone
2 Oct 2013	Weak westerly flow
12 May 2014	Southwest flow with coastal jet
22 Jul 2014	New York Bight Jet
23 Jul 2014 (flight 1)	New York Bight Jet (before jet)
23 Jul 2014 (flight 2)	New York Bight Jet (after jet)
31 Jul 2014	Southwest flow with coastal jet
11 Nov 2014	Cold northwest flow over warmer coastal waters

et al. (2013) found relatively good agreement between the WRF and buoy observations over the outer continental shelf of the western Atlantic. Nunalee and Basu (2014) used a coastal radiosonde and profiler to show that the strength of an LLJ case in WRF near New York City was sensitive to the PBL parameterization and initial atmospheric conditions used but less sensitive to the sea surface temperatures and vertical model resolution. For extreme low wind speeds, the Coupled Boundary Layers Air–Sea Transfer (CBLAST; Edson et al. 2007) field experiment collected data around Nantucket island during the midsummer period during 2001–03 in order to improve models. The CBLAST observational tower extended to 24 m MSL, with additional turbulence, wind, and temperature data obtained by Long-EZ aircraft flights and SODAR.

The field campaign reported on here, Improving the Mapping and Prediction of Offshore Wind Resources (IMPOWR), addresses CBLAST deficiencies using data from a taller, 60-m tower as well as other observations within the PBL. The Cape Wind (CW) meteorological tower, located within Nantucket Sound (Fig. 1), was operational from 2003 to 2011 and recorded data at multiple levels (20, 41, and 60 m). A goal of IMPOWR is to collect observations to validate and improve the boundary layer parameterizations in models, especially during stable marine conditions.

The IMPOWR field program began in fall 2012 and continued through summer 2015, extending the analysis begun by CBLAST both geographically and seasonally. The goals of this paper are to provide an overview of the IMPOWR experiment and to describe a few case studies to further motivate the research. The cases illustrate a coastally enhanced flow event near Nantucket island and a New York Bight jet along the New Jersey coast.

**IMPOWR DESIGN. Observations.** A number of different in situ observational datasets were used during the IMPOWR experiment. Surface observations over the coastal waters were obtained from the National Data Buoy Center’s moored buoys and Coastal Marine Automated Network stations, while surface land observations were available from National Weather Service (NWS) Automated Surface Observing System stations (Fig. 1a). Except for the NWS radiosondes over eastern Long Island [Upton, NY (OKX)] and coastal Massachusetts [Chatham (CHH)], which provided 12-hourly observations of temperature, moisture, and winds throughout the PBL, all other datasets were at a single fixed height. Through a partnership with CW, historical data from the CW meteorological mast (Figs. 1b,d) were acquired, consisting of continuous 10-min observations of wind speed and direction at

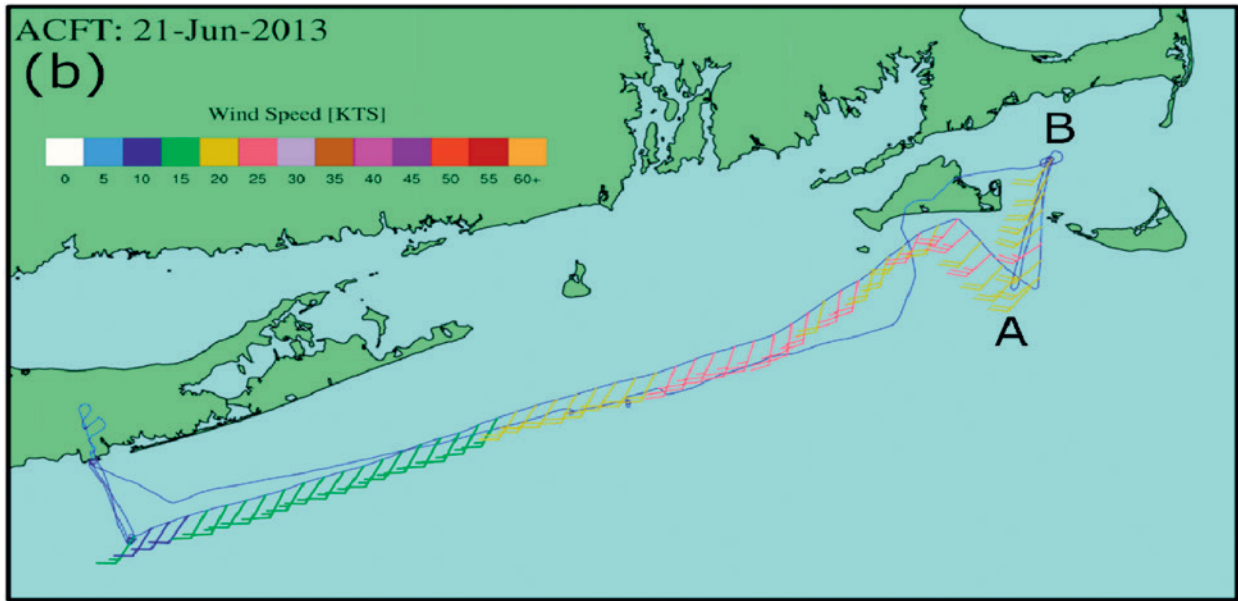
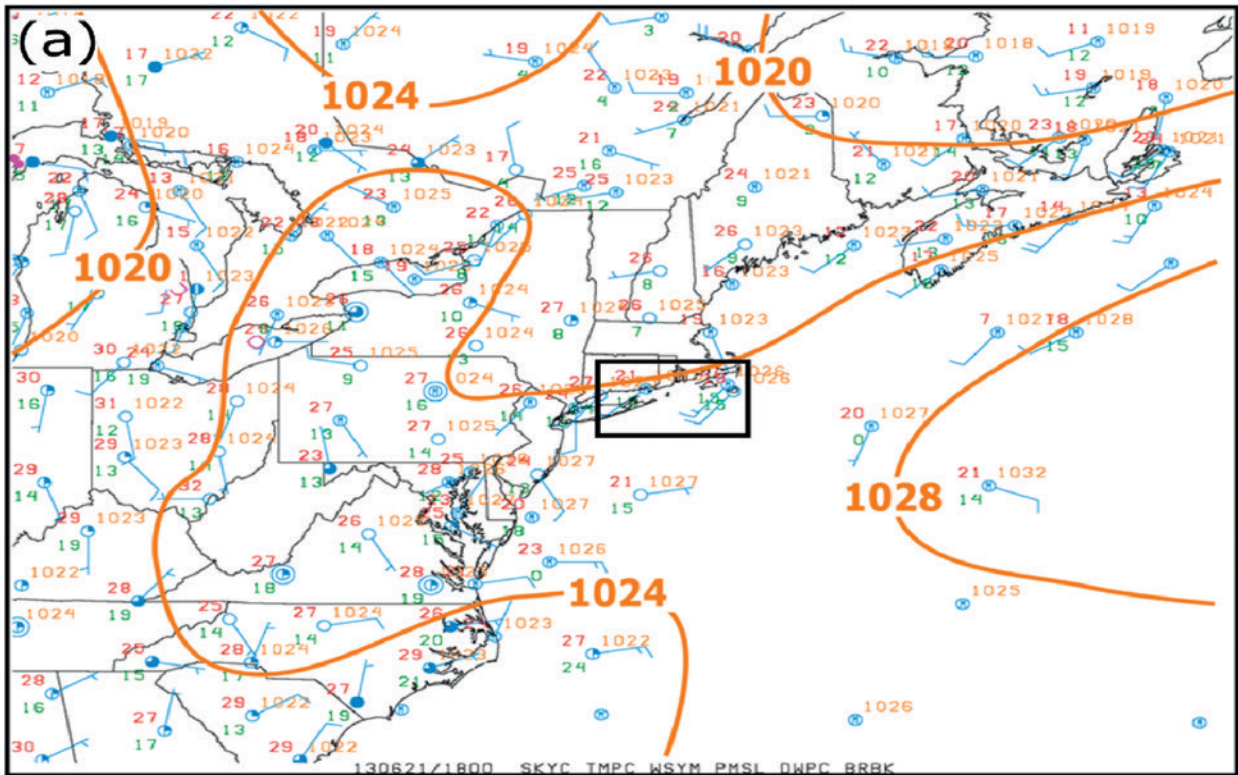


**FIG. 4.** (a) Surface analysis over the Northeast United States and mid-Atlantic from the National Oceanic and Atmospheric Administration (NOAA) Weather Prediction Center at 1800 UTC 21 Jun 2013, with sea level pressure contoured every 4 hPa. (b) Wind speed from the Long-EZ flight track at 40–50 m [colored in knots (kt;  $1 \text{ kt} = 0.51 \text{ m s}^{-1}$ )] and each full barb is  $5 \text{ m s}^{-1}$ . The box in (a) is the location of the flight level data in (a).

20, 41, and 60 m and temperature and pressure at 10 and 55 m above the sea surface over Nantucket Sound during 2003–11. As depicted in Fig. 2a, there is a strong seasonal cycle in wind speed at the CW tower, with the average winds gradually decreasing during the spring and early summer months, as diurnal

circulations dominate synoptically driven systems, followed by a rapid increase of wind speed in October, as the synoptic pressure gradients increase. The winds at all three levels follow the same annual cycle, but the winds at 60 m are generally 10%–20% faster than at 20 m. Wind directions at the 20-m level of

the CW tower have a strong seasonal signal too (Fig. 3), with southwesterly winds prevailing in the summer as a result of circulation around the offshore Bermuda high, while more frequent cold-air outbreaks from the North American continent result in more westerly to northwesterly winds during the winter.

At the start of the IMPOWR project, the CW instrumentation was no longer recording data, so the platform of the CW tower (~10 m MSL) was instrumented with wind, temperature, and relative humidity sensors at two locations, about 2 m above the platform; a high-speed optical wave gauge was also installed. The data were recorded continuously at 20 Hz and transmitted from the tower every 10 min. IMPOWR measurements were taken at the CW tower for about two years (April 2013–December 2014), although not continuously. Because of the limited power storage in the solar batteries, the system had to run on a

6-h reduced power cycle in the winter months; in addition, because of the loss of connectivity at the CW tower, no recording is available during July 2013 and 2014. The average wind speed from the IMPOWR sensors (Fig. 2a) shows very similar seasonal patterns to the historical data as well as to the nearby buoy 44020 (shown for the same sampling period as the IMPOWR data). The strong correlation between wave height and 10-m wind speed is also documented in Fig. 2b. Additional observations at 25 m MSL were available at the Buzzard's Bay tower operated by the National Oceanic and Atmospheric Administration and at 24 m at the air–sea interaction tower (ASIT) that had also been used in the CBLAST experiment (ASIT in Fig. 1a). Finally, two lidars (from Deepwater Wind, LLC) were deployed in the summer of 2014 at Southampton on Long Island and at the southwest corner of Block Island to get continuous wind measurements from 18 to 150 m above the surface.

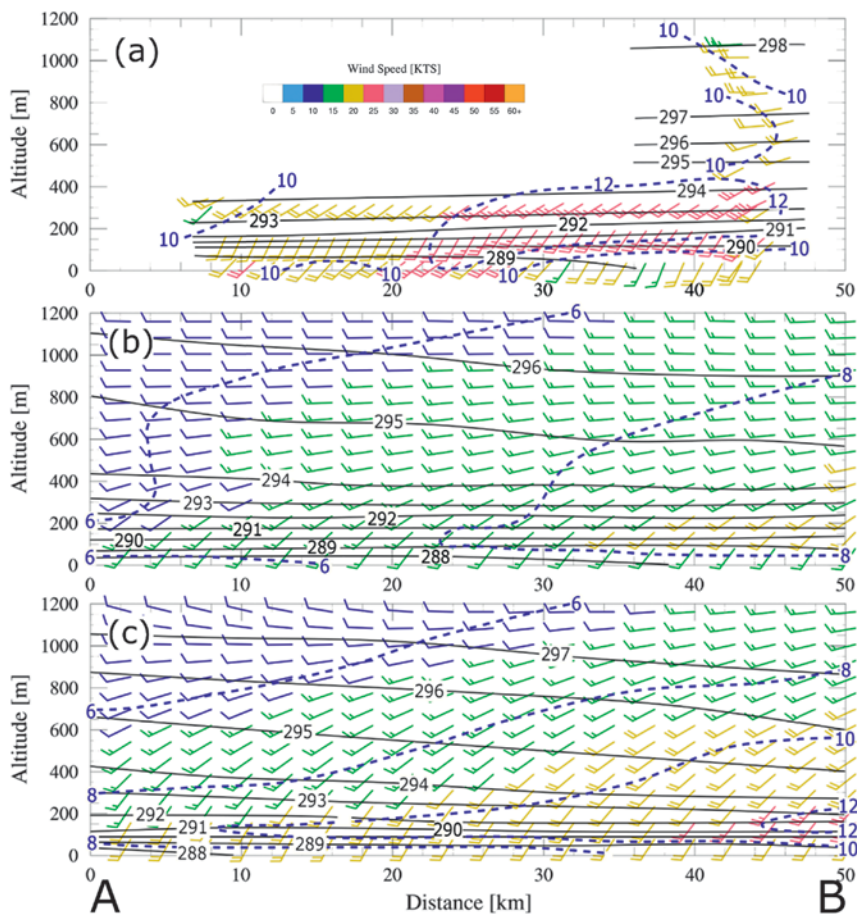


**FIG. 5.** (a) Potential temperature (contoured every 1 K), wind barbs (full barb = 10 kt or  $\sim 5 \text{ m s}^{-1}$  using the color bar in Fig. 3), and wind speed (every  $2 \text{ m s}^{-1}$ ) from the Long-EZ observations along AB shown in Fig. 3. (b) As in (a), but for the 1.33-km WRF at 1800 UTC 21 Jun (forecast hour 18). (c) As in (b), but for the 1.33-km WRF at 2100 UTC.

Aircraft flights were conducted as part of the IMPOWR field campaign during the spring and summer of 2013 and 2014. A Long-EZ aircraft was used during 2013 (Fig. 1c), while a Cozy Mark IV aircraft was used after the fall of 2014 (not shown). Both aircraft were fitted with the Aircraft Integrated Meteorological Measurement System (AIMMS-20) instrument, which is capable of recording observations of three-dimensional winds, temperature, pressure, and relative humidity at a frequency up to 40 Hz. Flight operations were based out of Brookhaven Airport (KHVV in Fig. 1a) and targeted the coastal areas of Nantucket Sound, Buzzard's Bay, and Block Island Sound, as well as the New Jersey coast. Various flight maneuvers, such as constant-level flight legs, spiral soundings in the lowest 2 km, and slant-sounding flight legs below 1 km, were conducted in order to provide marine boundary layer profiles of momentum, thermal, and moisture fields, as well as turbulence and

flux quantities. A typical flight involved about an hour of transport to the location, around 2 h of sampling, and then the return flight to eastern Long Island.

**WRF setup.** The Advanced Research version of the WRF (ARW; Skamarock et al. 2008) Model, version 3.4.1, was used for a series of short-term (30 h) runs for two separate evaluation periods: the historical period centered on the available data from the Cape Wind Meteorological Mast (2003–11) and the IMPOWR aircraft flights conducted in 2013/14. This paper focuses on the simulations for the IMPOWR flights, in which a large 4-km domain was used as the outer domain over the Northeast United States, eastern Great Lakes, and Atlantic coastal waters, with a one-way, nested, inner 1.33-km domain (Fig. 1 region). The WRF Model employed the Yonsei University (YSU; Hong et al. 2006) PBL parameterization, unified Noah land surface scheme (Tewari et al. 2004), Rapid Radiative Transfer Model (RRTM) longwave radiation (Iacono et al. 2000), Dudhia shortwave radiation (Dudhia 1989), and Thompson microphysical parameterization (Thompson et al. 2004, 2008), with no convective scheme on either domain. The initial and lateral boundary conditions were supplied by hourly analyses of the National Centers for Environmental Prediction's Rapid Refresh (RAP; Benjamin et al. 2009). The RAP was chosen for the WRF simulations of the flight cases because of its higher spatial and temporal resolutions, as well as improved data assimilation methods, relative to other available gridded analyses. The 1/12° daily gridded sea surface temperature (SST) product

from the National Centers for Environmental Prediction was prescribed for all WRF runs. The model output interval for the 1.33-km domain was increased to 5 min in order to allow for interpolation of the model variables to the aircraft position in time and space.

**FIELD EXAMPLES.** As of early 2015, there have been 18 flights using the Long-EZ aircraft (Table 1). We sampled a variety of different flow regimes, with a focus on the diurnal coastal flows during the warm season. There were several southwesterly flow cases, with enhanced flows and jets near the coast, but also two offshore (westerly) or northeasterly flow events. All events had limited low cloud cover during the daytime (typically afternoon), which allowed more focus on the dry PBL processes during diurnal heating. Good visibility allowed the aircraft to descend to and sample 30–50 m above the sea surface.

Three example cases are discussed below to highlight the data collected as well as to show preliminary comparisons with the WRF Model. These events have enhanced southerly or southwesterly flow, with two events to the east of Long Island on 21 June 2013 and 31 July 2014 and a New York Bight jet event on 23 July 2014.

**21 June 2013 Nantucket event.** Three flights were conducted in the 4-day period of 20–23 June 2013, in the afternoons and evenings of 20, 21, and 23 June. The prevailing winds in the vicinity of Nantucket Sound during this period were predominantly south-southwesterly, with the presence of a high pressure center to the south and east (Fig. 4a), which increased in intensity throughout the period (not shown). By early afternoon (1800 UTC 21 June), the air temperatures increased to 28°–29°C over the interior of New England, while the air temperatures over the coastal waters measured by the buoys were 18°–19°C. As a result, the strongest southerly surface flow was 5–7 m s<sup>-1</sup> near the coast, while the winds were lighter and more variable over the interior land areas as well as farther offshore.

The Long-EZ aircraft took off at 1730 UTC 21 June and ferried to the

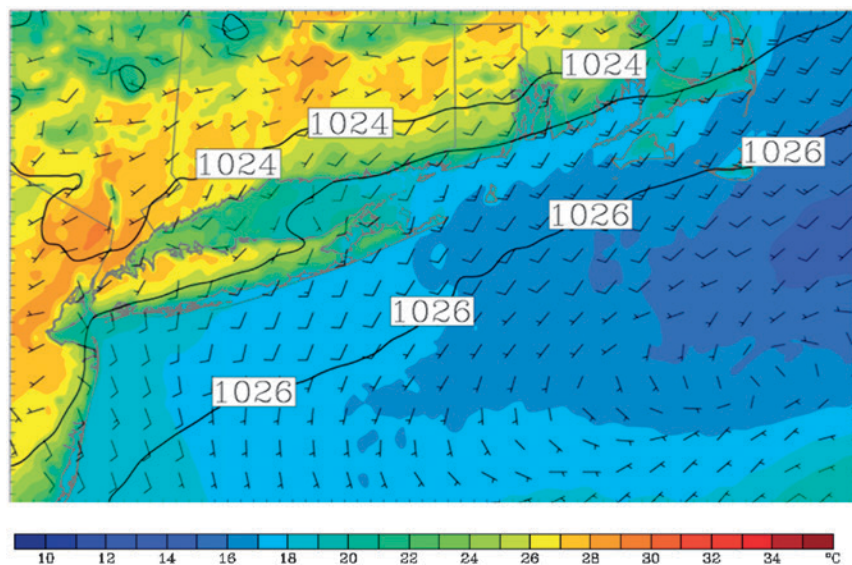


**FIG. 6.** The 1.33-km WRF surface (2 m) temperature (shaded; °C), sea level pressure (solid; every 1 hPa), and 50-m winds (full barb = 10 kt or ~5 m s<sup>-1</sup>) valid at 1800 UTC 21 Jun 2013 (forecast hour 18).



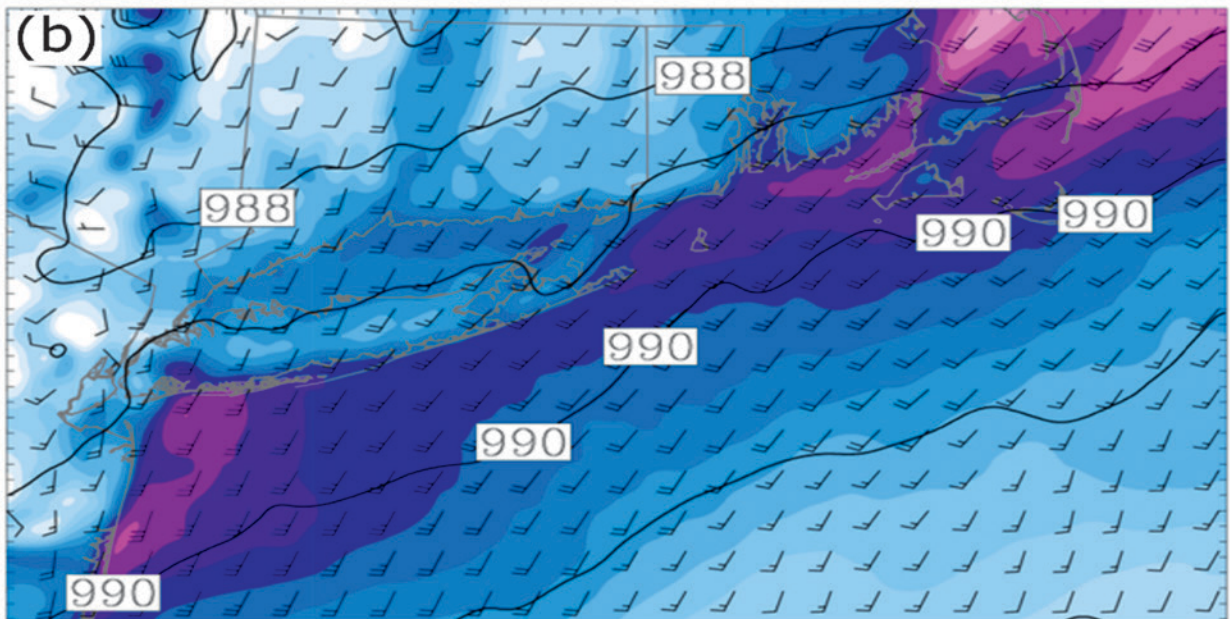
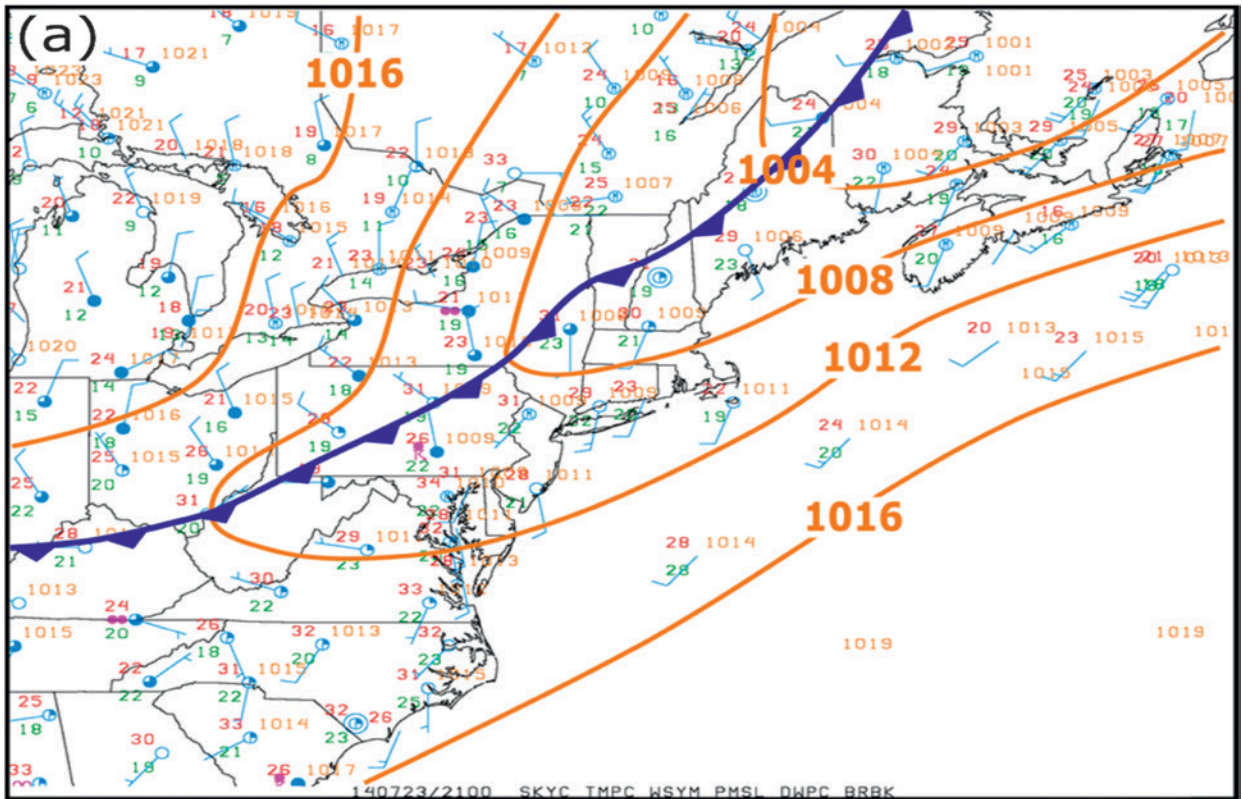


**FIG. 7.** (a) Surface analysis over the Northeast United States and mid-Atlantic from the NOAA Weather Prediction Center at 2100 UTC 21 Jul 2014, with sea level pressure (contoured every 4 hPa). (b) The 1.33-km WRF wind speeds at 180 m (shaded;  $\text{m s}^{-1}$ ; 1 full barb = 10 kt or  $\sim 5 \text{ m s}^{-1}$ ) at 2100 UTC 23 Jul (forecast hour 21).

Nantucket area while remaining nearly parallel to eastern Long Island (Fig. 4b). It completed a series of short north–south stacks and a profile near the CW

tower before returning back to Long Island following a similar track. Figure 4b shows the winds at about 50 m as the aircraft went toward Nantucket Sound.

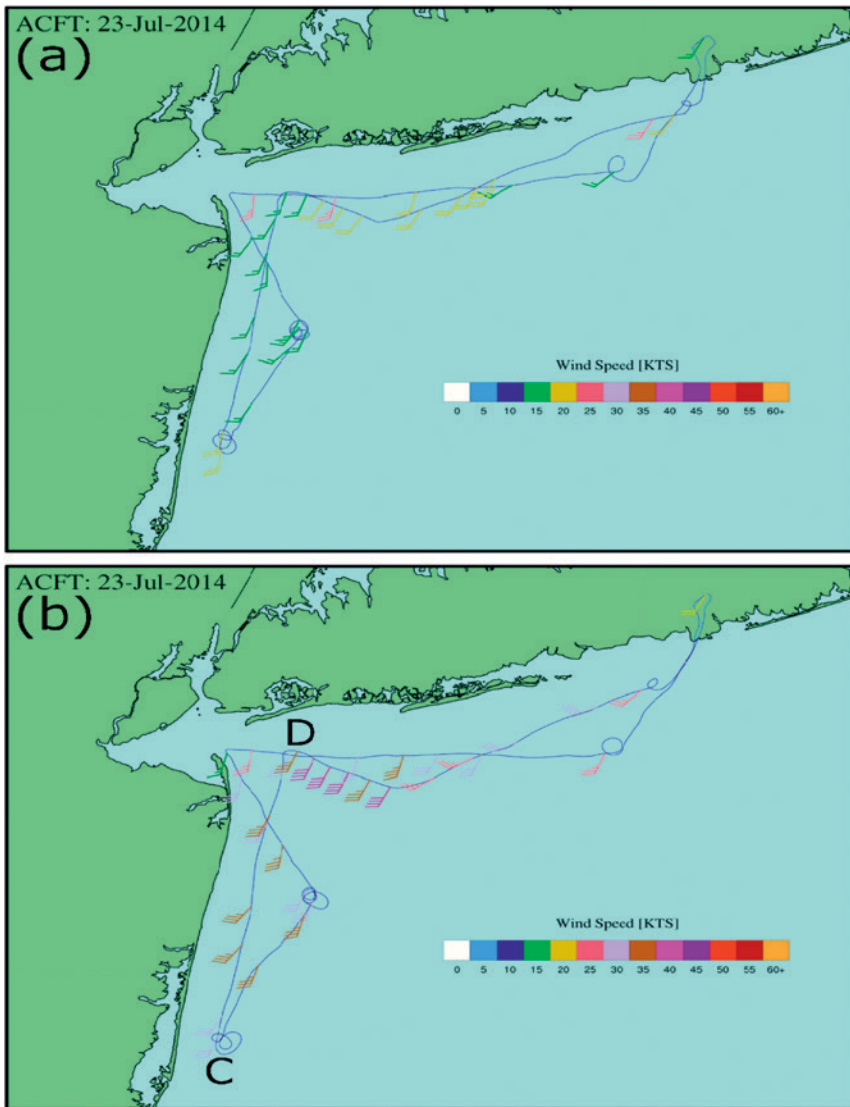


**FIG. 8. Flight track and flight-level winds (colored; kt; a full barb  $\sim 5 \text{ m s}^{-1}$ ) between 100 and 225 m MSL from the Long-EZ aircraft for (a) flight 1 from 1400 to 1700 UTC 23 Jul and (b) flight 2 from 2000 to 2200 UTC 23 Jul 2014.**

There was a steady increase in wind speeds from 8 to  $12 \text{ m s}^{-1}$  toward the east, which is suggestive of coastal enhanced low-level southerly flow. Figure 5a shows an analysis of the winds and potential temperatures for the north–south stacks into and out of Nantucket Sound and the spiral at CW. The observed static stability (vertical potential temperature gradient) is largest to the south and strongest around 150 m; this stable layer weakens and increases in height to the north. This is consistent with SST differences increasing from south to north, ranging from about  $16^\circ\text{C}$  just south of Nantucket Sound to about  $20^\circ\text{C}$  inside the sound (not shown). The observed marine layer in the observations is deeper over the northern half of the cross section, which hydrostatically enhances the surface pressure

difference between these coastal water locations and the interior land areas, thus resulting in enhanced flow ( $11\text{--}13 \text{ m s}^{-1}$ ) compared with locations to the south.

The WRF simulation with the YSU PBL is compared with the aircraft observations 18–21 h into the forecast at 1.33-km grid spacing. At 1800 UTC (Fig. 6), the WRF Model diurnally warms the interior up to  $28^\circ\text{C}$  at the surface; the surface winds are  $5\text{--}8 \text{ m s}^{-1}$  near the coast (Fig. 4a), while only  $2\text{--}3 \text{ m s}^{-1}$  south of Long Island, which is nearly  $4 \text{ m s}^{-1}$  weaker than the buoy observations. For the north–south cross section (Fig. 5b), the WRF isentropes are relatively flat at low levels with no evidence of a well-defined marine layer, and as a result, the winds are  $2\text{--}3 \text{ m s}^{-1}$  weaker than observed. The WRF Model does develop a more defined stable layer eventually by 2100 UTC (Fig. 5c), but the layer is very thin, extending from the surface to about 100 m, and the modeled winds are  $1\text{--}2 \text{ m s}^{-1}$  weaker than the 1800 UTC observations over the center

part of the cross section. Overall, the WRF Model developed the enhanced winds too slowly and the strongest winds are located too close to the coast.

**23 July 2014 New York Bight jet event.** Two flights occurred on 23 July 2014 to observe the development of the New York Bight jet along the New Jersey (NJ) coast toward western Long Island. At 1800 UTC 23 July, there was surface high pressure offshore of the U.S. East Coast (Fig. 7a), and there was a cold front over central New York (NY) and Pennsylvania that was progressing eastward. The surface temperatures ahead of this front around New York City (NYC) were  $32^\circ\text{--}33^\circ\text{C}$ , while they were  $24^\circ\text{--}25^\circ\text{C}$  over the coastal waters. WRF simulates a similar large-scale pressure

and surface temperature distribution across the region (not shown). In the 1.33-km WRF domain, the winds at 180 m MSL are 14–15 m s<sup>-1</sup> along the NJ coast at 2100 UTC (Fig. 7b), and there were also enhanced southerly winds just south of Long Island and along coastal southeast New England. This wind enhancement is similar to the simulated New York Bight jet enhancement in the WRF simulations presented by Colle and Novak (2010). This earlier study had limited observations to show the evolution of the jet.

Figure 8 shows the two flight tracks for sampling the jet as well as the along-track winds plotted when the aircraft was between 100 and 225 m MSL. During the first flight between 1400 and 1700 UTC 23 July (Fig. 8a), wind speeds are 5–10 m s<sup>-1</sup> from the southwest along the NJ coast. There is a slight enhancement in the wind speed to 10–12 m s<sup>-1</sup> in the New York Bight region and just south of Long Island. A north–south cross section for the leg parallel to the NJ coast shows a stable layer in the lowest 300 m (Fig. 9a), where there is a 4–5-K increase in potential temperature from 150 to 300 m; there is a mixed layer (nearly constant potential temperature) above this stable layer. This mixed layer was likely advected from the heated continental land areas (southern New Jersey). The winds in the section are strongest near the surface (~10 m s<sup>-1</sup>), with little evidence of enhanced flow from south to north at this time.

During the second flight between 2000 and 2200 UTC 23 July, much stronger winds were observed along the NJ and Long Island coasts (Fig. 8b). Wind speeds were 12–15 m s<sup>-1</sup> over much of the region, with the strongest winds (17–20 m s<sup>-1</sup>) over parts of the New York Bight. The south–north cross section (Fig. 9b) shows that the marine layer had increased in depth and was sloping down toward the north, with the strongest stability around 200–250 m MSL, especially in the northern part of the section. The winds had increased during the last few hours, with the largest wind speeds at 21 m s<sup>-1</sup> centered around 150 m MSL. The wind speeds increased 3–4 m s<sup>-1</sup> from

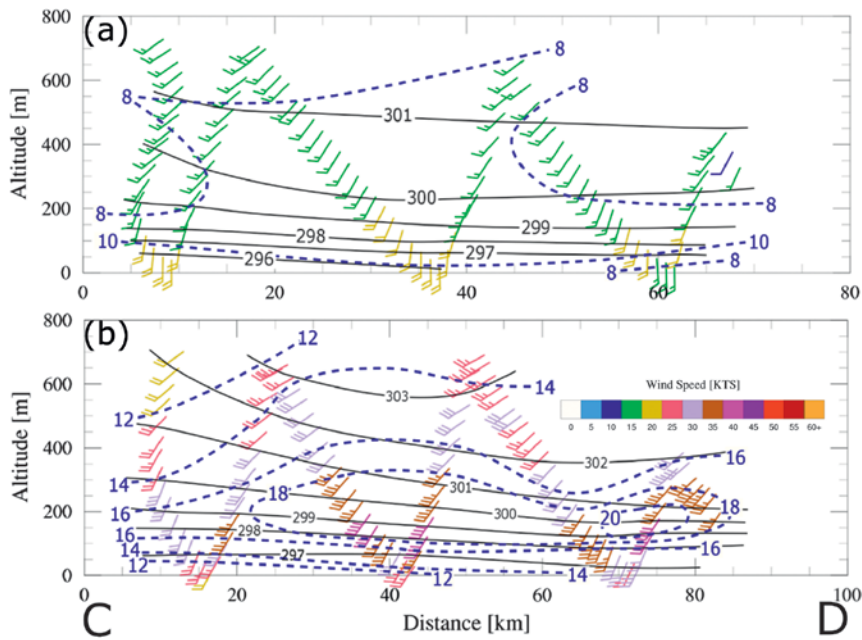


**FIG. 9.** (a) Potential temperature (contoured every 2 K), wind barbs (colored; kt; full barb ~5 m s<sup>-1</sup>), and wind speed (dashed blue; every 2 m s<sup>-1</sup>) from the Long-EZ observations along track CD shown in Fig. 8b from 1604 to 1623 UTC 23 Jul 2014. (b) As in (a), but for flight 2 in Fig. 8b from 2123 to 2141 UTC 23 Jul.

south to north over a 60–70-km distance at this level, with most of the change in the first 30 km. Overall, the magnitude of these gale force winds was unexpected, especially considering they were 5–6 m s<sup>-1</sup> stronger than the models predicted (Fig. 7b).

**31 July 2014: Low-level jet just east of Long Island.** On 31 July 2014, there was surface high pressure (~1,020 hPa) centered just east of the mid-Atlantic coast (not shown), which resulted in large-scale southerly flow across Long Island and southern New England. The surface wind increased from 3 to 5 m s<sup>-1</sup> in the morning over the coastal waters to 5–8 m s<sup>-1</sup> by late afternoon (not shown). The Long-EZ flew along the south coast of Long Island and measured southerly wind speeds from 7 to 8 m s<sup>-1</sup> at about 30 m MSL to 10 to 11 m s<sup>-1</sup> at about 700 m MSL.

The lidar on Block Island (cf. Fig. 1) provides more temporal detail of the winds for this event from 18 to 150 m above ground level (AGL; Fig. 10). There is an increase in the wind speed from about 7 m s<sup>-1</sup> between 100 and 150 m AGL around 1800 UTC 31 July 2014 to 9–10 m s<sup>-1</sup> by 2300 UTC 31 July, with the peak winds between 2300 UTC 31 July and 0400 UTC 1 August 2014. Colle and Novak (2010) also showed this early evening wind maximum using buoy observations in this region, which is important for wind power generation since it occurs near hub height.

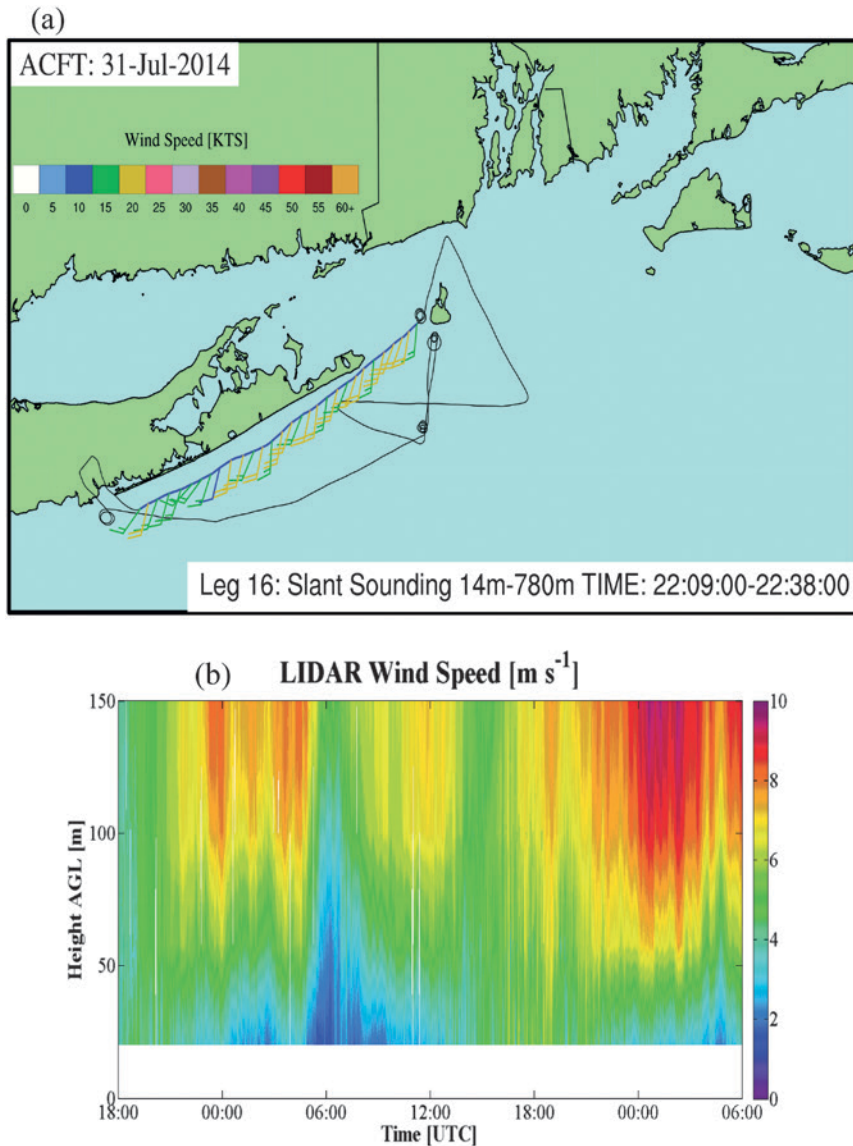


**FIG. 10. (a) Flight track and flight-level winds (shaded; kt; full barb  $\sim 5 \text{ m s}^{-1}$ ) between 30 and 700 m MSL from the Long-EZ aircraft for 2209–2238 UTC 31 Jul 2014. The location of the lidar is given by the Block Island (BI) location. (b) Lidar wind speed (shaded;  $\text{m s}^{-1}$ ) from 1800 UTC 30 Jul 2014 to 0600 UTC 1 Aug 2014.**

**SUMMARY AND RESEARCH OPPORTUNITIES.** The IMPOWR field study was motivated by the lack of thermodynamic and wind observations above 25 m MSL within the boundary layer over the Northeast U.S. coastal ocean. This has hindered the evaluation and improvement of planetary boundary layer parameterizations in these marine environments, which are important for wind resource assessment and forecasting in the coastal zone. The large number of days sampled with aircraft and other instruments during IMPOWR offers numerous scientific research opportunities. The IMPOWR campaign data are available by request on

the data archive and portal (DAP) of the Department of Energy (at <https://a2e.pnnl.gov/study>).

One major question is whether mesoscale models (e.g., WRF) can accurately simulate the wind and temperature profiles in the marine boundary layer under different synoptic flow conditions. Preliminary results from IMPOWR, as shown above for the 21 June 2013 and 23 July 2014 events, suggest that WRF underpredicts the amplitude of coastal low-level jets in this region and that these jets do not extend offshore enough and are too shallow in the model. There are several other IMPOWR jet events that can be evaluated to generalize these results (Table 1). In addition, several years (2003–11) of wind observations at Cape Wind tower from 20 to 60 m have been collected to investigate the wind profile from the surface to about wind turbine hub height. This CW data and the two coastal lidars over coastal Long Island and Block Island (cf., Fig. 1) will be used to better understand the wind profiles near hub height and can be compared with the models. For example, over 90 historical WRF simulations have been

completed using five different PBL parameterizations to construct a longer-term validation of WRF using these historical datasets, which will be reported in subsequent papers.

Another important question is what factors may be leading to the wind and temperature biases in the model? The WRF Model was rerun using several other PBL parameterizations for the two IMPOWR cases presented above as well as a few other events. Although there are some variations between the schemes, they all underpredict the warm-season low-level jets, which suggests that there are other factors

that may be limiting the jet magnitude than the turbulent closure assumptions in the PBL schemes. For example, the sea surface temperatures in WRF are fixed and based on an SST product that averages a few days of satellite-derived temperatures and buoys. In reality, the SSTs in Nantucket Sound can increase by 2°–3°C during afternoon heating and can exhibit significant spatial variability near the coast. As a result, the WRF SSTs tend to be too cool during the day, which may be leading to the cool bias in all PBLs, so additional experiments are needed to determine the role of these temporal and spatial SST variations on the simulated diurnal circulations.

IMPOWR also provides useful observations to test the importance of initial conditions and mesoscale data assimilation in the coastal zone, where there are relatively sparse data to properly initialize the model. If the spread in low-level winds in WRF using these different analyses (North American mesoscale model analysis, Rapid Refresh analysis, Global Forecast System analysis, and North American Regional Reanalysis) is larger than using different WRF PBLs for a single initialization, this suggests the importance of initial conditions to these coastal wind and temperature structures. The additional observations from IMPOWR can also be ingested into WRF using an ensemble Kalman filter approach (Evensen 2003), which would test the importance of data assimilation for these coastal flows.

Last, the IMPOWR dataset is helping to expand our understanding of important structures and processes associated with coastal diurnal flows that had only been modeled in previous studies (e.g., Colle and Novak 2010). For example, IMPOWR observations are yielding important knowledge on the small-scale variations in the marine boundary layer, such as localized pressure gradient and wind enhancements, similar to those observed in the 21 June and 23 July cases above. The derived turbulent kinetic energy (TKE) from these events will help determine the importance of vertical mixing even when the marine PBL is stratified with a relatively cool SST.

The value of these IMPOWR observations, consisting of both in situ aircraft and long-term in situ observations, will not only lead to improved boundary layer parameterizations over the coastal ocean, but also hopefully motivate additional field campaigns along the U.S. East Coast to tackle other conditions. For example, the Long-EZ aircraft could not fly at night or low levels with a relatively low cloud ceiling, so a moist PBL and turbulence cannot be addressed with IMPOWR. This is important given the relatively large wind resource in these areas and the general lack of model evaluations at hub height.

**ACKNOWLEDGMENTS.** We thank the three anonymous reviewers for their constructive comments that helped improve this manuscript. We acknowledge the support of the Department of Energy (DE-EE0005377) for this research. The authors thank Energy Management, Inc., developer of Cape Wind, for providing access to its offshore meteorological tower for our instruments and to the historical dataset from that tower. We also thank Deepwater Wind, LLC, for use of two lidars for this project and AWS\_Truepower for installing and maintaining these lidars.

## REFERENCES

- Archer, C. L., and Coauthors, 2014: Meteorology for coastal/offshore wind energy in the United States: Recommendations and research needs for the next 10 years. *Bull. Amer. Meteor. Soc.*, **95**, 515–519, doi:10.1175/BAMS-D-13-00108.1.
- Benjamin, S. G., and Coauthors, 2009: Technical review of Rapid Refresh/RUC project. NOAA/ESRL/GSD Internal Review, 168 pp.
- Bonner, W. D., 1968: Climatology of the low level jet. *Mon. Wea. Rev.*, **96**, 833–850, doi:10.1175/1520-0493(1968)096<0833:COTLLJ>2.0.CO;2.
- Carvalho, D., A. Rocha, M. Gomez-Gesteira, and C. Santos, 2014a: Sensitivity of the WRF model wind simulation and wind energy production estimates to planetary boundary layer parameterizations for onshore and offshore areas in the Iberian Peninsula. *Appl. Energy*, **135**, 234–246, doi:10.1016/j.apenergy.2014.08.082.
- , —, —, and —, 2014b: Comparison of re-analyzed, analyzed, satellite-retrieved and NWP modelled winds with buoy data along the Iberian Peninsula coast. *Remote Sens. Environ.*, **152**, 480–492, doi:10.1016/j.rse.2014.07.017.
- Colby, F. P., Jr., 2004: Simulation of the New England sea breeze: The effect of grid spacing. *Wea. Forecasting*, **19**, 277–285, doi:10.1175/1520-0434(2004)019<0277:SOTNES>2.0.CO;2.
- Colle, B. A., and D. R. Novak, 2010: The New York Bight jet: Climatology and dynamical evolution. *Mon. Wea. Rev.*, **138**, 2385–2404, doi:10.1175/2009MWR3231.1.
- Doyle, J., and T. Warner, 1991: A Carolina coastal low-level jet during GALE IOP 2. *Mon. Wea. Rev.*, **119**, 2414–2428, doi:10.1175/1520-0493(1991)119<2414:ACCL LJ>2.0.CO;2.
- Dudhia, J., 1989: Numerical study of convection observed during the Winter Monsoon Experiment using a mesoscale two-dimensional model. *J. Atmos. Sci.*, **46**, 3077–3107, doi:10.1175/1520-0469(1989)046<3077:NSOCOD>2.0.CO;2.

- Dvorak, M. J., B. Corcoran, J. Ten Hoeve, N. McIntyre, and M. Jacobson, 2012a: US East Coast offshore wind energy resources and their relationship to peak-time electricity demand. *Wind Energy*, **16**, 977–997, doi:10.1002/we.1524.
- , E. D. Stoutenburg, C. L. Archer, W. Kempton, and M. Z. Jacobson, 2012b: Where is the ideal location for a US East Coast offshore grid? *Geophys. Res. Lett.*, **39**, L06804, doi:10.1029/2011GL050659.
- Edson, J. B., and Coauthors, 2007: The Coupled Boundary Layers and Air–Sea Transfer Experiment in Low Winds (CBLAST-LOW). *Bull. Amer. Meteor. Soc.*, **88**, 341–356, doi:10.1175/BAMS-88-3-341.
- Evensen, G., 2003: The ensemble Kalman filter: Theoretical formulation and practical implementation. *Ocean Dyn.*, **53**, 343–367, doi:10.1007/s10236-003-0036-9.
- Hahmann, A. N., C. L. Vincent, A. Peña, J. Lange, and C. B. Hasager, 2015: Wind climate estimation using WRF model output: Method and model sensitivities over the sea. *Int. J. Climatol.*, **35**, 3422–3439, doi:10.1002/joc.4217.
- Helmis, C. G., Q. Wang, G. Sgouros, S. Wang, and C. Halios, 2013: Investigating the summertime low-level jet over the East Coast of the USA: A case study. *Bound.-Layer Meteor.*, **149**, 259–276, doi:10.1007/s10546-013-9841-y.
- Hong, S.-Y., Y. Noh, and J. Dudhia, 2006: A new vertical diffusion package with an explicit treatment of entrainment processes. *Mon. Wea. Rev.*, **134**, 2318–2341, doi:10.1175/MWR3199.1.
- Hughes, C. P., and D. E. Veron, 2015: Characterization of low-level winds of southern and coastal Delaware. *J. Appl. Meteor. Climatol.*, **54**, 77–93, doi:10.1175/JAMC-D-14-0011.1.
- Iacono, M. J., E. J. Mlawer, S. A. Clough, and J.-J. Morcrette, 2000: Impact of an improved longwave radiation model, RRTM, on the energy budget and thermodynamic properties of the NCAR Community Climate Model, CCM3. *J. Geophys. Res.*, **105**, 14873–14890, doi:10.1029/2000JD900091.
- Kempton, W., C. L. Archer, A. Dhanju, R. W. Garvine, and M. Z. Jacobson, 2007: Large CO<sub>2</sub> reductions via offshore wind power matched to inherent storage in energy end-uses. *Geophys. Res. Lett.*, **34**, L02817, doi:10.1029/2006GL028016.
- Manwell, J., A. Rogers, J. McGowan, and B. Bailey, 2002: An offshore wind resource assessment study for New England. *Renew. Energy*, **27**, 175–187, doi:10.1016/S0960-1481(01)00183-5.
- Monaldo, F. M., X. Lui, W. Pichel, and C. Jackson, 2014: Ocean wind speed climatology from spaceborne SAR imagery. *Bull. Amer. Meteor. Soc.*, **95**, 565–569, doi:10.1175/BAMS-D-12-00165.1.
- Musial, W., and B. Ram, 2010: Large-scale offshore wind power in the United States: Assessment of opportunities and barriers. National Renewable Energy Laboratory Rep. NREL/TP-500-40745, 240 pp.
- Novak, D., and B. A. Colle, 2006: Observations of multiple sea breeze boundaries during an unseasonably warm day in metropolitan New York City. *Bull. Amer. Meteor. Soc.*, **87**, 169–174, doi:10.1175/BAMS-87-2-169.
- Nunalee, C., and S. Basu, 2014: Mesoscale modeling of coastal low-level jets: Implications for offshore wind resource estimation. *Wind Energy*, **17**, 1199–1216, doi:10.1002/we.1628.
- Ryan, W. F., 2004: The low level jet in Maryland: Profiler observations and preliminary climatology. Maryland Department of the Environment, Air and Radiation Administration Tech. Rep., 43 pp.
- Skamarock, W. C., and Coauthors, 2008: A description of the Advanced Research WRF version 3. NCAR Tech. Note NCAR/TN-475+STR, 113 pp., doi:10.5065/D68S4MVH.
- Tewari, M., and Coauthors, 2004: Implementation and verification of the unified Noah land surface model in the WRF Model. *20th Conf. on Weather Analysis and Forecasting/16th Conf. on Numerical Weather Prediction*, Seattle, WA, Amer. Meteor. Soc., 14.2A. [Available online at [https://ams.confex.com/ams/84Annual/techprogram/paper\\_69061.htm](https://ams.confex.com/ams/84Annual/techprogram/paper_69061.htm).]
- Thompson, G., R. M. Rasmussen, and K. Manning, 2004: Explicit forecasts of winter precipitation using an improved bulk microphysics scheme. Part I: Description and sensitivity analysis. *Mon. Wea. Rev.*, **132**, 519–542, doi:10.1175/1520-0493(2004)132<0519:EFOWPU>2.0.CO;2.
- , P. R. Field, R. M. Rasmussen, and W. D. Hall, 2008: Explicit forecasts of winter precipitation using an improved bulk microphysics scheme. Part II: Implementation of a new snow parameterization. *Mon. Wea. Rev.*, **136**, 5095–5115, doi:10.1175/2008MWR2387.1.
- Woods, B. K., T. Nehr Korn, and J. M. Henderson, 2013: A downscaled wind climatology on the outer continental shelf. *J. Appl. Meteor. Climatol.*, **52**, 1878–1890, doi:10.1175/JAMC-D-12-0216.1.
- Zhang, D., S. Zhang, and S. Weaver, 2006: Low-level jets over the mid-Atlantic states: A warm season climatology and a case study. *J. Appl. Meteor. Climatol.*, **45**, 194–209, doi:10.1175/JAM2313.1.